Geochemistry Geophysics Geosystems G3
AN ELECTRONIC JOURNAL OF THE EARTH SCIENCES
Published by AGU and the Geochemical Society

Article
Volume 10, Number 11
17 November 2009
Q11010, doi:10.1029/2009GC002702
ISSN: 1525-2027

Stagnant lid convection and carbonate metasomatism of the deep continental lithosphere

Norman H. Sleep
Department of Geophysics, Stanford University, Stanford, California 94305, USA (norm@stanford.edu)

[1] The current (and past) mantle adiabat beneath continents is hot enough that ascending carbonate-rich domains partially melt liberating kimberlites. Over the last 2 Ga, most of these kimberlites have been trapped and frozen in the deep continental lithosphere, forming a massive CO_2 reservoir. Geochemical studies of kimberlites that reached the surface indicate the pervasiveness of their effects within the deep lithosphere. These magmas extensively reacted with the deep lithosphere on the way up. Conversely, studies of deep mantle xenoliths brought up in kimberlites detect repeated episodes of metasomatism by these fluids. The heat balance between convection and conduction through the lithosphere provides gross constraints on the cumulative global effects of this process. Stagnant lid (including chemical lid) convection supplies heat to the base of continental lithosphere in equilibrium with the conductive heat flow. The thermal gradient beneath continents is constrained by xenolith geotherms and mantle heat flow q is $\sim$20 mW m^{-2}. The upwelling velocity V at the base of the thermal boundary layer is $\sim q/T_\eta \rho C$, where ρC is volume specific heat, 4 MJ m^{-3} and T_η is the temperature to change viscosity by a factor of e, $\sim$60 K. The upwelling velocity is thus $\sim$2 km per million years; the mass of the mantle circulates beneath continents over $\sim$2 Ga. The rate that plate tectonics recirculates the mantle is comparable and limits the supply carbonate-rich undepleted material to the melting zone of upwelling stagnant lid convection and thus the production of kimberlites. Overall the amount of CO_2 emplaced by kimberlites into continental lithosphere is a significant fraction ($\sim$1/2) of that in the convecting mantle, resulting in a major deep lithospheric reservoir of CO_2 of $\sim 5000 \times 10^{18}$ moles, an equivalent thickness of $\sim$2 km carbonatized rock. This process, however, is insufficient to affect the overall density of deep lithosphere. The observed linearity of the xenolith geotherm precludes equivalent thicknesses of several kilometers depending on the radioactive element concentration of actual kimberlites. Kimberlites are partial melts often of subducted carbonatized oceanic crust and hence have CO_2 to radioactive element ratios higher than the bulk mantle. Most kimberlites remain within the deep lithosphere because ascending dikes do not usually penetrate the region of horizontal compression in the strong cool part of the lithosphere. Conversely stresses relax quickly within the warm deep lithosphere allowing dikes to repeatedly intrude.

Components: 11,333 words, 5 figures.

Keywords: kimberlite; carbon dioxide cycle; lithosphere; xenolith; convection; craton.

Index Terms: 1038 Geochemistry: Mantle processes (3621); 8120 Tectonophysics: Dynamics of lithosphere and mantle: general (1213); 8125 Tectonophysics: Evolution of the Earth (0325).

Received 6 July 2009; **Revised** 1 October 2009; **Accepted** 8 October 2009; **Published** 17 November 2009.

Sleep, N. H. (2009), Stagnant lid convection and carbonate metasomatism of the deep continental lithosphere, *Geochem. Geophys. Geosyst.*, *10*, Q11010, doi:10.1029/2009GC002702.

1. Introduction

[2] The adiabatic ascent of the mantle provides a petrological construct for understanding the generation of basalt at ridge axes [e.g., *McKenzie and Bickle*, 1988; *Plank and Langmuir*, 1992; *Asimow*, 2002]. The base of the lithosphere truncates the adiabatic column when material ascends beneath midplate regions. Once formed and segregated, magmas ascend and interact with the overlying lithosphere. This processes modifies the compositions of lavas that eventually reach the surface [*Francis and Patterson*, 2009] and metasomatizes the lithosphere along its path [*Foley*, 2008; *De Stefano et al.*, 2009]. In particular, CO_2-rich melts from the base of the column including kimberlites (*sensu lato*) form lithospheric carbonates that may subsequently remelt [*Tappe et al.*, 2008]. They may even change the density and other macroscopic properties of the lithosphere [*Foley*, 2008; *Francis and Patterson*, 2009]. The purpose of this paper is to apply physics and mass balance to constrain the gross extent of this process. The arguments strive where possible for factor of two constraints with the intent of obtaining the order of magnitude of the carbonate reservoir in the deep continental lithosphere. They do not depend strongly on detailed geochemistry. Hence, many geochemical details are beyond the scope of this paper. I flag rounded estimates where they arise but retain extra digits where I may aid in following calculations or in comparing related quantities.

2. Overview of Carbonate-Rich Mantle Melts

[3] The idea that CO_2-rich mantle domains melt at great depths to produce low-volume alkalic rock types has been widely studied by petrologists. For example, such melts laterally remove highly incompatible elements from the ascending region beneath ridge axes, and hence cause mid-ocean ridge basalt (MORB) that melts from the typical residuum to be depleted in these elements [*Donnelly et al.*, 2004]. Conversely, CO_2-rich magmas locally contaminate MORB [*Dasgupta et al.*, 2009]. Deep CO_2-rich melts metasomatize overlying regions of the Hawaiian plume affecting rejuvenated stage lavas [*Dixon et al.*, 2008]. Previously intruded lithospheric dike networks remelt during rifting [*Tappe et al.*, 2008].

[4] *Francis and Patterson* [2009] presented a model for the generation of deep continental alkalic magmas. They divide these rocks into two classes. (1) Kimberlites (type 1, *sensu stricto*) erupt preferentially within cratons. They attribute these CO_2-rich melts to interaction of initially CO_2-rich sublithospheric melts with the overlying highly depleted lithosphere. (2) Aillikites erupt preferentially in noncratonic environments. They interact with less depleted "ordinary" mantle to produce magmas with a lower CO_2 content. Both these processes (if sufficiently pervasive) change the density and other material properties of the gross lithosphere. Sections 3 and 4 present heat and mass balance arguments that these changes to the lithosphere are in fact likely to be widespread enough that the deep lithosphere is a globally significant CO_2 reservoir. I use "kimberlite" in its general sense unless otherwise indicated to avoid introducing unfamiliar rock names and awkward collective nouns.

3. Global Mantle Carbon Cycle and Reservoirs

[5] I briefly review the mantle carbon cycle to put the kinematics of stagnant lid convection in context. From top down, the relatively simple kinematics of ridges allows geochemists to estimate the current flux of CO_2 from the mantle and the bulk CO_2 in the Earth's mantle. Next there are plenty of divalent cations within the deep lithosphere to potentially sequester massive reservoirs of CO_2. Third, the bulk of the mantle's carbon entered it by subduction of very carbon-rich domains. Subsequent melting of these domains moves carbon around but leaves new carbon-rich domains in its wake.

3.1. Mantle Carbon Reservoir

[6] Geochemists distinguish the high CO_2 content of the domains that actually melt at great depth from the much lower bulk average CO_2 of the mantle. Modern estimates of the latter parameter utilize ratios, including $CO_2/^3He$ and CO_2/Nb, and focus on mid-oceanic ridge axes including transform faults that sample voluminous pooled magmas [e.g., *Saal et al.*, 2002; *Cartigny et al.*, 2008]. Such estimates are conveniently given in terms of fluxes per year from ridge axes and then extrapolated to the rest of the mantle assuming mantle-wide convection. I assume to get the estimates in a common form that a volume of $\sim$162 km^3 a^{-1} melts beneath ridge axes. (3 km^2 a^{-1} for new seafloor area with melting to 50 km beneath the base of 6 km thick crust [*Plank and Langmuir*, 1992]; the mass of the mantle 4×10^{24} kg

circulates through this zone every 7 Ga at the current rate.)

[7] Estimates obtained in this manner have somewhat greater than a factor of 2 range. *Saal et al.* [2002] estimate a ridge flux of 0.9×10^{12} mol a^{-1} giving 72 ppm mantle concentration that extrapolates mantle wide to 6500×10^{18} moles, equivalent to CO_2 pressure of 56.5 bars. *Cartigny et al.* [2008] prefer 2.3×10^{12} mol a^{-1}, giving 184 ppm mantle concentration, $16{,}700 \times 10^{18}$ moles, and equivalent CO_2 pressure of 144 bars. *Hirschmann and Dasgupta* [2009] critically reviewed these estimates. Their estimate range is $9750 \pm 4200 \times 10^{18}$ moles. The center of this range is equivalent to 85 bars or 108 ppm.

[8] For comparison, crustal sediments store 7100×10^{18} moles, equivalent to 62 bars of CO_2, 1/5 of which by mole is organic carbon and the remaining 4/5 carbonate [e.g., *Holser et al.*, 1988]. *Hirschmann and Dasgupta* [2009] preferred a similar estimate of 7750×10^{18} moles. Reservoir mass estimates are useful for computing the amount of carbonate emplaced into the lower lithosphere and visualizing its global significance. The residence time necessary for a given process to recirculate the bulk the mantle is a kinematic measure that does not involve element concentrations.

3.2. Potential Carbonate Sink in Deep Lithosphere

[9] There are plenty of divalent cations in mantle peridotite to potentially accumulate massive amount of carbonates in the lower lithosphere. In particular, magnesite $MgCO_3$ is a stable phase in equilibrium within peridotite [e.g., *Dasgupta and Hirschmann*, 2007]. A generic peridotite with a density of 3400 kg m^{-3} and 75% by weight Mg_2SiO_4 provides a quantitative example. An idealized reaction is

$$\text{(R1)} \qquad CO_2 + Mg_2SiO_4 \Rightarrow MgCO_3 + MgSiO_3;$$

[10] Carbon dioxide in melt + Olivine in rock $\Rightarrow$ Magnesite in rock + Orthopyroxene in rock. Thus each mole of olivine can consume 1 mol of CO_2.

[11] For visualization, I use equivalent thicknesses to express volumes of material emplaced in the lithosphere. I do not imply that actual thin layers exist. Carbonates from intrusion and metasomatism may well be distributed over a depth range of several 10s of km. Carbonation of even a small fraction of this potential depth range has a huge effect on the global carbon ledger. For example, an equivalent thickness of 1.25 km of peridotite thus can consume a (rounded) weight per area of 100 bars (10^6 kg m^{-2}) of CO_2. As the continents cover 40% of the Earth's surface, formation of 3.125 km equivalent thickness of carbonated peridotite beneath continents would sequester a global equivalent of 100 bars or 11000×10^{18} moles.

[12] This amount provides a generic example of the implications of the lower continental lithosphere being a carbon reservoir comparable to the crust and the mantle. Overall, the formation and delivery of CO_2-rich magmas to the deep lithosphere as opposed to the availability of divalent cations in peridotite governs whether a massive CO_2 reservoir exists in that region. Still, the typical effect on density is likely to be modest. The 3.125 km equivalent thickness of carbonated peridotite to globally sequester 100 bars of CO_2 produces a minor change in overall lithospheric density. MgO-related density differences occur over a much larger depth range in the lithosphere as discussed in section 5.

3.3. Subduction of Carbon

[13] Carbon subduction delivers very carbon-rich domains to the mantle. The main subduction component is carbonatized uppermost oceanic basalt. (That is, layer 2A in traditional ridge nomenclature. Seismologists originally defined this layer by its very low seismic velocity compared with low-porosity basalt. Carbonates form near the base of this layer at ~0.5 km depth within highly porous buried lava flows that are cut by some dikes.) Some pelagic carbonates and organic carbon sediments also subduct with the slab. Studies of volcanic gases confirm that this material actually subducts and that some of it quickly returns to the surface at island arcs [e.g., *Sano and Williams*, 1996].

[14] The long-term (100s Ma) average of deep subduction is relevant to the mantle budget. The instantaneous flux depends on vagaries: whether pelagic carbonates form, the total CO_2 concentration in the ocean that determines the rate of crustal carbonate formation, and rate that organic carbon rich sediments make it to trenches. Overall, CO_2 subduction flux estimates depend on the observation that significant masses of carbon remain both in sediments and in the mantle. The net flux of carbon into the deep mantle by subduc-

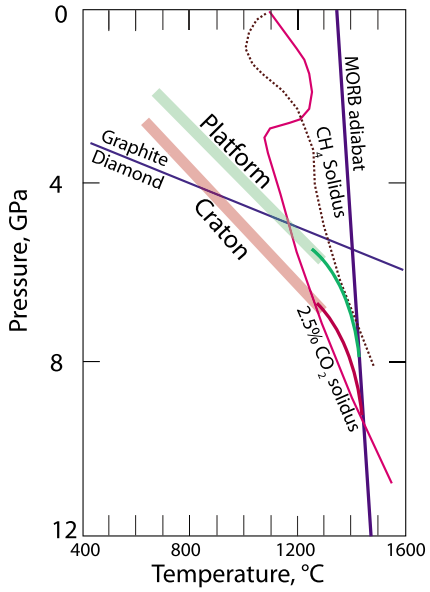

Figure 1. Petrological grid shows diamond-graphite stability line, MORB adiabat, the CO_2-rich solidus, and the CH_4 for mantle rocks. Xenolith studies yield the conductive geotherm in a platform and a cratonal location (thick lines drawn through arrays of points determined from individual samples). The geotherm is expected to curve from the conductive gradient to the adiabatic gradient within the rheological boundary layer (thin solid lines). The petrological studies did not obtain xenoliths from this depth range, nor compile data from the shallow lithosphere. Note that carbonate is stable from the base of the lithosphere to the left of the melting curve to its kink at ~3 Ga (~100 km). Carbonates decompose at magmatic temperatures at shallower depths. Modified after *Francis and Patterson* [2009].

tion is comparable to the ridge flux but not as well constrained.

[15] The bulk of the Earth's carbon was subducted into concentrated mantle domains early in its history [*Sleep et al.*, 2001; *Zahnle et al.*, 2007]. The Moon-forming impact left the interior of the Earth molten and too hot to initially subduct carbonates. The Earth's carbon formed a dense ~200 bar, hot ~500 K CO_2 atmosphere. The Earth's environment became clement when subduction sequestered this CO_2 into the mantle. Limited recent ^{142}Nd data from an alkalic complex in India [*Upadhyay et al.*, 2009] bear on the timing of this event and the chemical durability of mantle carbon-rich domains. That is, the measurements relate to the antiquity of subduction. The straightforward interpretation of these data is that carbonate-rich oceanic upper crust formed and was subducted at ~4.26 Ga; a melt from this domain intruded the Indian lithosphere at ~3.6 Ga, and the intruded material remelted to become part of a shallow alkalic complex at ~1.48 Ga.

[16] Note that subduction produces a chemical variety carbonatized crust, with basalt-hosted systems currently the most likely. Some serpentinite-hosted domains likely form at ultraslow ridge axes and near fracture zones. Komatiite-hosted domains likely formed on the early Earth. Once suducted, carbon remains in concentrated domains unless it reaches the near surface in a voluminous melt. Formation of low-volume melts from the subducted domains and their entrapment elsewhere in the mantle has the net effect of replacing slab-hosted carbon-rich domains with ambient mantle and lithosphere hosted carbon-rich domains.

4. Convective Transfer of Mantle Carbon Into Melting Zones

[17] Metasomatism of the deep lithosphere by melts derived from ascending stagnant lid convection is qualitatively attractive because it provides a continual protracted source of fluids. Careful studies of diamonds and xenolith suites record multiple events over the life of the lithosphere as well as diamonds derived from deeply ascending material [e.g., *Foley*, 2008; *De Stefano et al.*, 2009].

[18] The phase relationships indicate that carbonate-rich domains ascending on a platform or craton geotherm will melt (Figure 1). I presume that the carbonate-rich material mostly melts and that the bulk of this melt initially ascends. Thus the long-term rate where convection delivers mantle to the melting zone is relevant to the amount of carbonate that has accumulated in continental lithosphere.

[19] In particular, the flow field is time dependent and material at the mantle adiabat is stirred through the melting zone more than once. Kinematically, the positions of upwellings and downwelling relative to overlying lithosphere move around and the convection pattern reorganizes as plate motions change. It is thus necessary to consider both the physics of stagnant lid convection that directly supplies material to the melting zone and the physics of plate-driven mantle-wide convection that control the replenishment rate of the upper asthenosphere.

4.1. Heat Flow at Base of Lithosphere

[20] I constrain the vigor of stagnant lid convection by noting it supplies heat to the base of the lithosphere that is in balance with conductive heat flow in the lithosphere. Analysis of xenolith geo-

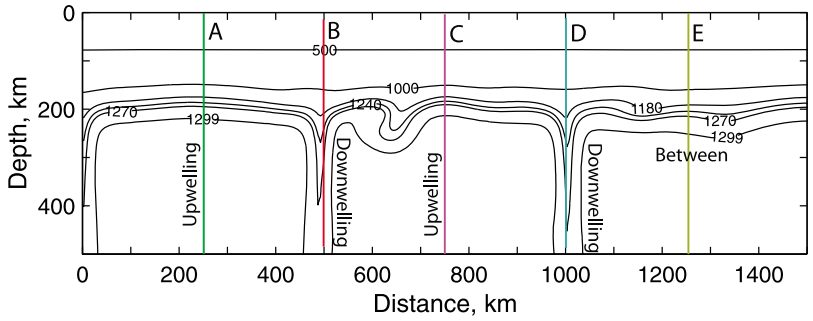

Figure 2. Computed potential temperature contours in degrees Celsius. Vertical lines show positions of geotherms in Figure 3. The abiabatic gradient is subtracted from the computed temperature. Most of the asthenospheric domain is within 1 K of the assumed mantle adiabat 1300°C. Modified after *Sleep* [2003a].

therms combined with phase relationships quantifies the heat flow and with analysis of the physics of convection the production rate of CO_2-rich melts beneath the lithosphere. The xenolith data in Figure 1 do not resolve the rheological boundary layer.

[21] Within resolution, the lithospheric geotherms in Figure 1 are linear as would be expected for steady state vertical conduction through a rigid medium with negligible radioactive heat generation and constant thermal conductivity. In general, the laterally averaged vertical conductive heat flow is

$$q_d = k\frac{\partial T}{\partial z} = k\frac{T_L}{Z_L}, \tag{1}$$

where k is thermal conductivity, T is temperature, and z is depth. The second equality implies that the xenolith geotherm extrapolates to the mantle adiabatic temperature T_L and the lithospheric scale depth Z_L.

[22] Convection in the mantle below the lithosphere balances the heat carried upward by conduction. At asthenospheric depths, convection dominates and the geotherm is essentially adiabatic except within downwellings (Figure 2). Both conduction and convection carry heat flow in the transition region between lithosphere and asthenosphere, called the rheological boundary layer. The laterally averaged heat flow is constant with depth at steady state

$$\langle q\rangle = \langle q_d\rangle + \langle q_v\rangle = k\frac{\partial\langle T\rangle}{\partial z} + \rho C\langle VT\rangle, \tag{2}$$

where angle brackets indicate lateral averaging, q_v is convective heat flow, ρ is density, C is specific heat per mass, and V is vertical velocity positive upward. The term $\langle VT\rangle$ is positive because hot buoyant material tends to rise and cold dense material tends to sink. It is convenient to express $\langle VT\rangle$ in terms of a scale velocity V and the typical change in temperature between upwellings and downwellings ΔT_{down}. Equation (2) is then

$$\langle q\rangle = k\frac{\partial\langle T\rangle}{\partial z} + f(z)\rho CV\Delta T_{\text{down}}, \tag{3}$$

where the function $f(z)$ varies smoothly and monotonically between 0 at the top of the rheological boundary layer to 1 at its base. Conversely the thermal gradient varies from the conductive value T_L/Z_L at the top of the thermal boundary layer and 0 (more precisely adiabatic) at its base (Figure 1).

[23] The fact that the conductive and convective terms in (3) are comparable within the thermal boundary layers leads to well known scaling relationships. First, one may solve for the scale velocity

$$V = \frac{\langle q\rangle}{\rho C\Delta T_{\text{down}}} \tag{4}$$

which applies within the boundary layer. The thickness of the boundary layer is

$$\Delta Z_{\text{rheo}} \approx \frac{2Z_L\Delta T_{\text{rheo}}}{T_L} \approx \frac{\kappa}{V}, \tag{5}$$

where $\Delta T_{\text{rheo}} > \Delta T_{\text{down}}$ is the full temperature contrast across the boundary layer, the factor of $\sim$2 arises because the thermal gradient changes smoothly from conductive to abiabatic within the boundary layer, and $\kappa \equiv k/\rho C$ is the thermal diffusivity.

[24] Note that the nonrheological physical parameters are adequately constrained. The numerical model in Figures 2 and 3 assumes the following: the thermal conductivity k = 3 W m^{-1} K^{-1}, the

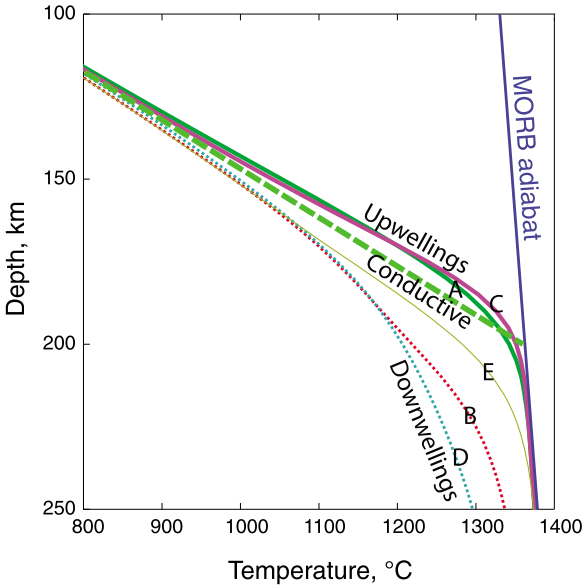

Figure 3. Computed geotherms in degrees Celsius. Vertical lines in Figure 2 show positions of geotherms. The geotherm in the upwellings approaches the mantle adiabat at the extrapolation of the conductive geotherm (thick dashed line). Modified after *Sleep* [2003a].

specific heat per volume is ρC = 4 MJ m^{-3} K^{-1}, the thermal diffusivity is then $\kappa = 0.75 \times 10^{-6}$ m^2 s^{-1}, the density is 3400 kg m^{-3}; and the thermal expansion coefficient is $\alpha = 3 \times 10^{-5}$ K^{-1} that is needed below. The acceleration of gravity used in the models is g = 9.8 m^2 s^{-1}. The numerical models assume that the MORB adiabat extrapolates to the rounded value 1300°C at the surface. The more sophisticated petrological grid in Figure 1 assumes 1350°C. The differences among the geotherms, melting curves, and the adiabat are relevant to the discussion, not their precise absolute values.

[25] The conductive heat flow in the models in Figures 2 and 3 is 19.5 mW m^{-3} and compatible with the xenolith geotherms in Figure 1. I acknowledge heat flow studies often give somewhat lower values for cratonal geotherms of 7 to 15 mW m^{-3} [e.g., *Jaupart et al.*, 1998; *Jaupart and Mareschal*, 1999; *Artemieva and Mooney*, 2001]. Geophysicists obtain these heat flow based estimates by subtracting an estimate of the heat flow generated by radioactive decay in the crust from the surface heat flow measured in boreholes. This method has the problem that the resulting mantle heat flow is the difference between 2 comparable larger numbers. A caveat is warranted, as a sampling problem exists. Carbonate-rich domains do not melt on the MORB adiabat if the lithosphere is too thick and the geotherm too cold (Figure 1), although ascending plume material might melt at a greater depth. I am not aware of xenolith geotherm data from an area of purported very low mantle heat flow.

4.2. Ascent Velocity Estimation

[26] Simple calculations show that the scale velocity V implies significant flow over geological time. To proceed, it is necessary to explicitly consider rheology and the detailed kinematics of the material that melts and the depleted material that then sinks. First, it is necessary to constrain ΔT_{down} to obtain the scale velocity V from (4). A simple expression for viscosity provides illustration

$$\eta = \eta_0 \exp\left[\frac{-\Delta T}{T_\eta}\right], \tag{6}$$

where η_0 is the viscosity at the mantle adiabat, ΔT is the temperature above the mantle adiabat, and T_η is the temperature scale for viscosity. Empirically, and $\Delta T_{\text{rheo}} \approx 2.4 T_\eta$ [*Davaille and Jaupart*, 1993a, 1993b, 1994; *Solomatov*, 1995; *Solomatov and Moresi*, 2000].

[27] Here the rate that convection feeds new undepleted material into the melting zone is relevant; one must avoid counting the same material twice. The position of upwellings and downwellings moves around with time so the instantaneous velocity is greater than that long-term supply velocity of deep undepleted material to the melting zone. Specifically, the instantaneous velocity just beneath the thermal boundary layer is greater than that predicted by (4) [*Sleep*, 2003a]. Downwellings cover only a limited ~0.1 part of the domain (Figure 2). Their velocity is hence ~10 times faster than the scale velocity. The downwellings entrain the surrounding adiabatic mantle causing its upward velocity to be also higher than that predicted by (4). The downward entrained material remains neutrally buoyant with respect to the ambient asthenosphere and is likely to be entrained upward again in time dependent flow.

[28] With regard to the temperature in the melting zone, the scale length κ/V within strong upwellings is thus much less than the predicted by (5). The computed ascending geotherm in strong upwellings, which is where melting should preferentially occur, approaches the intersection of extrapolation of the conductive geotherm with the adiabat (Figure 3).

[29] I obtain the supply velocity relevant to mass balance by noting that only material that cools

significantly in the thermal boundary layer sinks to great depth and hence is replaced with new undepleted material. The sinking material samples the temperature range in the boundary layer ΔT_{rheo}, but the average temperature deficit is less than this. I use $\Delta T_{\text{down}} \approx T_\eta$ on the grounds it is an average of the material when it starts down. Note that the actual value of ΔT_{down} is less than this where chemically buoyant lithosphere provides a lid to convection [e.g., *Sleep and Jellinek*, 2008].

[30] I present an example calculation. The value of T_η is somewhat constrained. Values from 100 K and 43 K (that implies a factor of 10 change over 100 K) are sometimes used in numerical calculations. I use $T_\eta = 60$ K from the models in Figures 2 and 3. The conductive heat flow in the models and from the xenolith geotherms in Figure 1 $\sim$19.5 mW m^{-3} provide the numerical example. The scale velocity is thus 2.6 km Ma^{-1}. This velocity is enough that the entire mass of the mantle (4×10^{24} kg) circulates beneath continents over 2200 Ma. There is hence kinematic opportunity for melting during stagnant lid convection to emplace massive carbonate deposits (comparable to the $\sim$100 bars of ambient CO_2 in the current mantle) into the lower continental lithosphere over geological time.

4.3. Mantle Supply Rate

[31] The estimate in the previous section assumed that the mantle is adiabatic so that the deep mantle replenished depleted material that sunk in downwellings. This assumption is appropriate for obtaining a local replenishment rate, but it is inappropriate on a billion year time scale.

[32] I present a quick example calculation based on the work of *Bunge* [2005]. The viscosity of the lower mantle is much greater than that of the upper mantle. Slabs pond near the base of the mantle and are not stirred back to the surface by the motions of surface plates and shallow slabs. Over a billion year time scale the material in previous slabs is displaced upward by new slabs and gradually ascends toward the surface.

[33] The old slab material heats up by radioactivity decay as it ascends. The secular cooling of the Earth's mantle over time acts as an additional virtual internal heat source. Hence the thermal gradient in the middle mantle is somewhat subadiabatic. The cool downwellings associated with stagnant lid convection sink to a level of neutral temperature and neutral buoyancy. Undepleted material cannot pass through the melting zone of stagnant lid convection faster than the gradual ascent of the deep mantle replenishes the upper asthenosphere.

[34] I obtain the gross rate that slabs recirculate the mantle using the current global seafloor spreading rate of 3 km^{-2} a^{-1}, density of 3400 kg m^{-3}, and an effective thickness the slab and its entrained material of 200 km. The yields a cycle time of 1960 Ga, comparable to the cycle time for stagnant lid convection. In more detail, slabs are composed of oceanic lithosphere and entrain undepleted material that has not had a chance to participate in stagnant lid convection beneath continents. The actual replenishment rate beneath continents is hence somewhat less than the replenishment rate associated with the cycle time obtained above. A detailed three-dimensional calculation with realistic plates, slabs, and continents with resolved stagnant lid convection is needed to get a precise answer. It would also need to keep track of the very long-term depletion of CO_2 in the mantle as it becomes sequestered in platform carbonates and the deep continental lithosphere and the replenishment of mantle CO_2 by subduction.

[35] Rather than attempting this task, I use the result that the plate and stagnant lid cycle times for the mantle are comparable $\sim$2 Ga so that the net emplacement of carbon into the continental lithosphere over its average age of $\sim$2 Ga is $\sim$1/2 of the raw estimate obtained by considering stagnant lid convection alone. In round numbers, my preferred estimate is 5000×10^{18} moles (43 bars), comparable but somewhat less the platform carbonate reservoir.

4.4. Comparison With Observed Kimberlite Flux

[36] Mass balance yields the global frequency of kimberlite intrusions needed to sequester, for an upper limit example, 100 bars global equivalent of CO_2 (10^6 kg m^{-2}). The Jericho kimberlite (*sensu stricto*) in the Slave Province of Canada provides data. The undegassed rock had $\sim$17% CO_2 by weight [*Price et al.*, 2000] so the global volume of kimberlite with a density of 3000 kg m^{-3} is 10^9 km^3. The equivalent thickness if equally distributed beneath continents is 2 km. The production rate extrapolated over 2.5 Ga is 0.4 km^3 a^{-1}.

[37] I make the trial assumption that this material all ascends in dikes that reach the surface to obtain an order of magnitude estimate. The observed along-strike distance of the Jericho-related dikes

of ~14 km [*Cookenboo*, 1999] provides an estimate of the volume of a successful extrusion [*Sleep*, 2003a]. The volume of a (rounded) 1 m wide dike extending down to 200 km depth is 2.8 km^3. From this reasoning, one would expect that an intrusion of kimberlite would occur somewhere on the Earth decanally to centennially, even if the total estimated emplaced volume is high by a factor of 10.

[38] The actual eruption rate of kimberlites is obviously much less than this. None are known to have erupted in historical time. Qualitatively, observations indicate that kimberlites in fact tend to be trapped at depth. In the model of *Francis and Patterson* [2009], those high CO_2 magmas that reach the surface interacted extensively with the lithosphere. The presence of clinopyroxene megacrysts in the Jericho kimberlite indicates that these magmas loitered in the deep lithosphere before they ascended [*Kopylova et al.*, 1999a, 1999b], as did southern African kimberlites [*Moore and Lock*, 2001]. See section 5.4 for a mechanical discussion of trapping at great depth.

[39] A caveat arises here. The kimberlites that reach the surface with this reasoning are a small fraction of the number that starts upward. The kimberlites that we can analyze are thus a biased sample. The petrologist can deduce the primary composition of the kimberlite magma to some extent, but to a large extent this is an unavoidable sampling problem.

5. Geodynamic Implications

[40] Assuming that the phase relationships in Figure 1 are properly calibrated, ascending CO_2-bearing material melts beneath both cratons and platforms. The solidus for mantle with 2.5% CO_2 is representative for this value down tiny ~5 ppm concentrations below which carbon resides in nominally C-free minerals [*Dasgupta and Hirschmann*, 2007]. This curve likely represents the true solidus for very CO_2-rich regions. However, laboratory magnesite-out temperature is then ~100 K higher. It is obvious that CO_2-rich melting would occur at greater depths in the past when the interior of the Earth was hotter and currently within mantle plumes that impinge beneath continents. Magnesium carbonate is a stable phase throughout most of the lithosphere. It will stay put unless heated by a subsequent event and assimilated by a carbonate unsaturated magma.

[41] Carbonates are unstable at low (that is crustal) pressures at the temperatures of ascending magmas and rapidly breakdown at reasonable ascent rates. The scarcity of carbonate in mantle xenoliths is likely to indicate this process, rather than indicate their absence in the deep lithosphere [*Canil*, 1990]. Note that graphite, unlike diamond, cannot be readily extracted by milling rock and there is no economic incentive to extract it. Hence this mineral tends to be undersampled and underreported in kimberlites and xenoliths (D. McKenzie, personal communication, 2004).

[42] The cratonal curve does not intersect the CH_4-rich solidus, implying as observed that diamonds do survive within locally reduced regions. The platform geotherm marginally intersects that solidus.

[43] One chemical and four geodynamic issues arise and are discussed in the remainder of this section. (1) Carbonate-rich domains are stable locally in the deep lithosphere and in the ascending mantle for melting begins. (2) Geophysicists may be marginally able to remotely observe carbonatized mantle. (3) Kimberlites carry the heat-producing radioactive elements Th, U, and some K. Xenolith geotherms provide a useful upper limit on the bulk concentration of kimberlites. (4) Most CO_2-rich magmas fail to reach the surface, as they would need to penetrate the rigid uppermost lithospheric mantle to do so. (5) Carbonate-rich domains may weaken the lithosphere. The fate of the water in kimberlites and its effects are mostly beyond the scope of this paper.

5.1. Stability of Carbonate in the Deep Lithosphere

[44] The stable carbon phase in the deep lithosphere is an issue. The purpose of this subsection is to show that carbonate can exist locally within the mantle lithosphere, given this inference that it occurs within very carbon-rich domains. My discussion follows a review paper by *Frost and McCammon* [2008]. Diamond (or graphite) is the stable carbon phase at the typical in situ oxygen fugacity of deep lithospheric xenoliths at pressures above ~4 GPa (~135 km depth). The thermodynamics though complicated in detail are straightforward. An idealized solid-state reaction is

$$4\mathrm{FeO\ (in\ rock)} + \mathrm{CO_2\ (in\ carbonate)} \Longleftrightarrow 2\mathrm{Fe_2O_3\ (in\ rock)} + \mathrm{C\ (diamond\ or\ graphite)}. \quad \text{(R2)}$$

The iron oxidation states Fe-II and Fe-III partition between multiple mineral phases in solid solution. At shallow depths, spinel (with Fe_3O_4 as a major component) bears the Fe-III. In the deep lithosphere, garnet bears the Fe-III as a minor component. This dilution reduces the activity of Fe-III driving the reaction to the right. Thus, the oxygen fugacity at constant composition decreases with depth along an adiabat in the deep lithosphere.

[45] However, the more abundant component in the bulk rock, either Fe or C, tends to buffer the oxidation state of the other scarcer component. Large additions of carbonate by a kimberlite and the carbonate-rich source regions locally overwhelm the local ambient Fe-II and so that carbonate minerals remain stable along with some elemental carbon. In terms of mass balance, a generic peridotite has ~10% FeO component by weight. Assuming a density of 3400 kg m^{-3}, a cubic meter of rock consumes 1.18×10^3 moles of CO_2 if reaction (R2) goes to completion. (It does not go to completion as the Fe-bearing components are in solid solution. This thermodynamic constraint does not modify the gross implications of the mass balance.) Addition or presence of much less than of 1.18×10^3 moles m^{-3} carbonate results in a reaction that is buffered through (R2) where a small fraction of the ambient Fe-II reacts to form elemental carbon. Complete carbonatization by reaction (R1) in contrast consumes the much larger amount of 1.82×10^4 moles m^{-3} of CO_2. Carbonate-rich kimberlite source regions by this reasoning have a higher oxygen fugacity than their surrounding ordinary mantle. So do domains with significant intrusion of kimberlites or CO_2 metasomatism. Solid carbonate-rich region can persist out of equilibrium with ordinary reducing mantle because chemical diffusion is extremely slow.

5.2. Density and Other Bulk Variations

[46] A generic peridotite with 75% Mg_2SiO_4 provides a numerical example of density change associated with carbonatization. The densities of the idealized phases in reaction (R1) are 3227, 3263, and 3010 kg m^{-3} for olivine, orthopyroxene, and magnesite, respectively [*Smyth and McCormick*, 1995, Table 1]. The density of the components in reaction (R1) decreases by 85 kg m^{-3} and the bulk density decreases by ~64 kg m^{-3}. This change is greater than negative thermal buoyancy in downwellings $\Delta\rho_T \approx \rho\alpha T_\eta = 6$ kg m^{-3}. It is comparable to the positive chemical buoyancy of cratonal lithosphere owing to its high Mg/(Mg + Fe) ratio. For example, *Griffin et al.* [1999] found 50 kg m^{-3} from analysis of xenoliths and melting relationships. *Doin et al.* [1997] used 60 kg m^{-3} in their numerical models. Geoid studies indicate that low-density region has an equivalent thickness of several 10s of kilometers and is not spatially resolved on this scale [*Shapiro et al.*, 1999a, 1999b]. This makes the similar additional density reduction by a few kilometers of equivalent thickness of carbonatized mantle futile to detect by gravitational methods. The uplift from carbonatization is below detection if occurs over geological time, for example, ~2% density decrease over 3 km causes only 60 m of uplift assuming isostasy. These conclusions carry through if dolomite $CaMg(CO_3)_2$ and/or aragonite $CaCO_3$ are actual carbonate phases. Their room condition densities are 2868 kg m^{-3} [*Smyth and McCormick*, 1995, Table 1] and 2930 kg m^{-3} [*Smyth and McCormick*, 1995, Table 1; *Bass*, 1995, Table 7], respectively. The density of diopside $CaMgSi_2O_6$ in comparison is 3279 kg m^{-3} [*Smyth and McCormick*, 1995, Table 1; *Bass*, 1995, Table 8].

[47] Seismic detection of carbonatized regions is appears difficult. The room temperature P wave velocity of magnesite is 8.25 km s^{-1} (parameters from *Bass* [1995, Table 3]). This value is similar to the velocity of mantle peridotites. The argument, however, does not consider anisotropy or hydrous phases formed from the water in kimberlites. *Snyder and Lockhart* [2009] suggest that observed deep lithospheric anisotropy in the Slave province, an area of abundant surface kimberlites, is associated with the intrusion of voluminous kimberlites at depth.

5.3. Radioactive Heat Generation and Thermal Gradient

[48] Xenolith studies constrain the geotherm and hence the concentration of heat-producing elements within the lithosphere. The concentration of radioactive elements in the Jericho Pipe kimberlite [*Price et al.*, 2000, Table 2] provides a useful starting example. I select this exposure, as data are available, with the caveat that its emplacement age is young and the rocks may not be representative of kimberlites over the last 2 Ga. The average abundance of K in pristine samples is ~0.3% by weight. The Th abundance is ~23 ppm. The U abundance was below the detection limit 1 ppm for most of their samples. The radioactive heat generation from Th dominates at $\sim 6.3 \times 10^{-10}$ W kg^{-1}. The heat generation from K is 0.1×10^{-10} W kg^{-1}. The

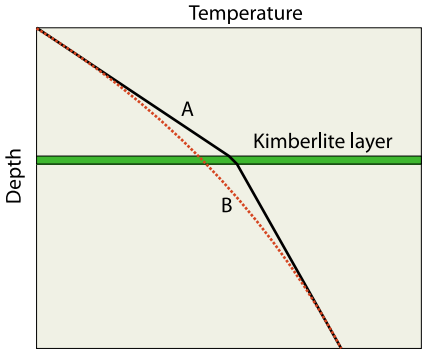

Figure 4. Schematic diagram of the effect of a radioactive region on the geotherm. A thin highly radioactive kimberlite layer (green) causes the geotherm (curve A) to be kinked. Radioactivity distributed over a broad depth range causes the geotherm to be curved (curve B).

detection limit of U would generate 1×10^{-10} W kg^{-1}. I use 7×10^{-10} W kg^{-1} and a density of 3000 kg m^{-3} to obtain 2×10^{-6} W m^{-3} for a generic numerical example.

[49] The ~2 km equivalent thickness of this kimberlite discussed in section 3.2 yields 4 mW m^{-2} of heat flow. The heat flow would increase upward by this amount within the region intruded by kimberlites (Figure 4). The generic heat flow of 19.5 mW m^{-2} and hence the thermal gradient changes by ~20%. This geotherm curvature would be evident in actual xenolith data that was used to compile Figure 1. Conversely, half this amount would be at the level of detection. That is, a kimberlite concentration equivalent to 10s of bars (5000×10^{18} moles) of CO_2 is compatible but not resolved by xenolith geotherms, but a significantly higher concentration is unlikely to be present where the geotherms are linear.

[50] This approach can be applied locally to the curvature or lack of curvature resolved by a xenolith geotherm. The typical concentration of radioactive elements in a CO_2-rich magma is variable and a meaningful average is not obvious. *Hoernle et al.* [2002] review oceanic carbonatites and compare them with continental ones. For example, the end-member oceanic carbonatite of *Dixon et al.* [2008, Table 7c] contains 40% CO_2 and only 3.35 ppm Th. Thus, one needs to consider the local kimberlites and their crystallization products to infer the concentration of radioactive elements the bodies that pond at depth.

[51] Overall, such work is complicated because U and Th partition into trace as well has major phases. For example, U tends to accumulate somewhat in zircon and strongly in baddeleyite rims from the breakdown of zircon and carbonate at shallow depths [*Davis*, 1977]. Conversely, study of zircons provides information on the Th/U ratio of the primary kimberlite. *Zartman and Richardson* [2005] obtained that this ratio decreased from its bulk earth value of ~4 to ~2 from 2.5 Ga to today as kimberlite source regions became more dominated by oxidized subducted material. They did not obtain absolute concentrations.

[52] I make quick estimates with data from mixed localities to illustrate how one would proceed with geochemical data specifically collected and analyzed for this purpose. I take the ratio Th/U 2 of modern kimberlites at face value. Then the analyzed Jericho kimberlite [*Price et al.*, 2000, Table 2] lost ~11 ppm of U by zircon crystallization which implies a radioactive heat generation of 5×10^{-6} W m^{-3} at the time that zircon commenced its crystallization. However, zircon appears late at ~90% crystallization in the sequence [*Zartman and Richardson*, 2005]. The primary magma heat generation was thus ~10% of the above amount or 0.5×10^{-6} W m^{-3}. In comparison, the end-member Hawaiian magma of *Dixon et al.* [2008, Table 7c] adjusting U so that Th/U is 2 has 0.7×10^{-6} W m^{-3} of heat generation. A 2 km equivalent thickness of the Jericho and the Hawaiian magmas yields 1 and 1.4 mW m^{-2} of heat flow, respectively, which would probably escape detection from xenolith geotherms. This argument does preclude an equivalent thickness of several kilometers. Further geochemical refinement is beyond the scope of this paper.

[53] Note that the direct effect of the intrusion of kimberlites into the lithosphere on heat flow is small. For a crude numerical example, an intruded kimberlite cools 500 K from its source temperature and latent heat is equivalent to another 500 K of cooling. The rock provides 4×10^9 J m^3. The intrusion of 1 km equivalent thickness of kimberlites over 1 Ga provides 0.1 mW m^{-3}, which is not resolvable.

5.4. Kimberlite Emplacement at Depth

[54] Assuming that kimberlites form dikes that just reach the surface aids in visualizing expected effects if eruption was in fact widespread. That is, the equivalent thickness of 2 km of kimberlite in the 200 km thick lithosphere corresponds to 1% of outcrop area if the bodies are turned on end as dikes. It is obvious that kimberlite outcrops are much less common that this.

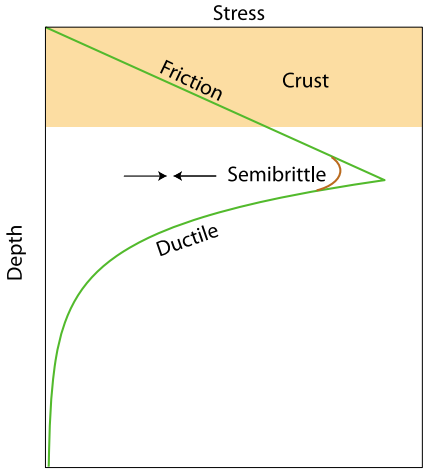

Figure 5. Schematic diagram of the expected deviatoric stress in stable continental lithosphere. Frictional failure controls the stress at shallow depth. Ductile creep at increasingly high temperatures controls the stress at great depths. The maximum stresses occur in between where both friction and creep lead to semibrittle behavior (red line). The horizontal stresses are typically more compressive than the vertical stresses. Dikes that ascend upward are thus diverted into horizontal sills.

[55] It is conceivable, however, that kimberlites typically make it nearly all the way to the surface so that the shallow strain occurs by extension of the country rock. In this case, one would expect contrary to observations that kimberlite would be common in deeply exhumed crust and uppermost mantle. This hypothesis may even have kinematic problems. The implied strain of 1% over 2.5 Ga yields a strain rate of 10^{-19} s^{-1}. The horizontal extensional strain rate in stable (low-heat flow) cratons is $\sim 10^{-20}$ s^{-1} from the observation that stresses from body forces like "ridge push" dominate over stresses which can relax including thermoelastic stress [*Zoback and Townend*, 2001]. A strain rate of 10^{-18} s^{-1} would produce unacceptable thickening or thinning of continental crust if it persisted over geological time [*Sleep and Zoback*, 2007]. Note that instantaneous geodetic measurements provide only the marginal constraint that the rate is less than 10^{-17} s^{-1} [e.g., *Calais et al.*, 2006].

[56] It is also conceivable that kimberlites do not efficiently segregate from the surrounding mantle. This is true to some extent with any low-fraction melt [e.g., *McKenzie*, 1984]. Enough carbon-rich melt remains in the oceanic asthenosphere to increase its electrical conductivity [*Gaillard et al.*, 2008]. However, there is much evidence that CO_2-rich melts are mobile relative to their surrounding mantle [*Dasgupta et al.*, 2009]. They extract enough material to affect the chemistry of more voluminous melts both in ridge [*Donnelly et al.*, 2004] and plume [*Dixon et al.*, 2008] settings.

[57] These inferences support the hypothesis that a significant part of the CO_2-bearing mantle carried upward by stagnant lid convection in fact forms kimberlites, but that these rocks intrude and freeze at deep lithospheric depths. This situation is expected from the mechanics of the lithosphere.

[58] At steady state, the lithosphere deforms horizontally over its full depth at a constant horizontal strain rate (Figure 5). This deformation generates little stress in the deep hot part of the plate and maintains the stress near frictional failure in the upper crust [*Zoback et al.*, 2002]. A deeper zone of very slow, ductile creep exists near the top of the lithospheric mantle within stable regions. The highest deviatoric stresses exist within this region. The horizontal membrane stress (difference between horizontal and vertical lithostatic stress) is typically compressive within stable continents [*Zoback et al.*, 1989, 2002]. The least compressive stress is the vertical lithostatic stress. These stresses result from "ridge push" so one can extrapolate the present to the past on the grounds that plate tectonics have occurred over that last 2 Ga.

[59] Ascending dikes intrude perpendicular to the least compressive stress. In the case of stable lithosphere, dikes encounter vertical least compressive stress as they approach the strong cold part of the lithosphere. These bodies become horizontal sills, cease to ascend, and quickly freeze. This reasoning also explains qualitatively why kimberlite intrusions are local and episodic rather than ubiquitous and continual since episodes of horizontal tension sometimes occur within usually stable continents and may lead to rifting.

[60] Conversely, the stress from dikes and sills emplaced within the deep lithosphere does relax quickly on a geological time scale, so that more dikes and sills can intrude later. The Maxwell time scale η/G where G is the stress modulus provides quantification. An asthenospheric viscosity of 0.657×10^{19} Pa s was used to compute Figures 2 and 3 (with forethought using the formula for *Davaille and Jaupart* [1993a, 1993b, 1994] for steady state heat flow, assumed to be 19.5 mW m^{-3}, in terms of physical constants including T_η = 60 K). The shear modulus of Mg-olivine is 81 GPA [*Bass*, 1995, Table 7]. The relaxation time is $\sim$2.5 a. Thus stresses relax (in thousands of years

giving time for many intrusions) within the rheological boundary layer and within the overlying regions where the viscosity in (6) is within a few orders of magnitude of that of the asthenosphere. This conclusion also holds for depleted Mg-rich cratonal lithosphere which is likely to be a factor of ~50 more viscous than ordinary mantle at given temperature and pressure [*Doin et al.*, 1997; *Sleep*, 2003b].

5.5. Weakening of the Lithosphere by Kimberlites

[61] *Tappe et al.* [2008] discuss the remobilization of CO_2-rich mantle during rifting. Lithosphere that has an exceptionally high concentration of kimberlites and carbonatized mantle may be prone to failure and more kimberlite intrusion [*Foley*, 2008]. Hydrous minerals derived from kimberlite water may be involved. The direct effect is that carbonates creep more easily than silicates, which is evident in metamorphic terrains. Dikes may provide throughgoing weak planes. The tendency for kimberlites of various ages to concentrate within particular regions like the Slave Province of Canada and Southern Africa bears on this issue with the caveat that mining interests may preferentially search near proven deposits.

[62] Radioactive heat generation has an indirect effect in that it increases the heat flow and thermal gradient. The temperature at a given depth is thus higher and the rocks weaker than in an unaffected area. The physics are analogous to the weakest link in a chain failing even if it only slightly differs from the rest of the links. *Perry et al.* [2006] discuss a case involving crustal compression along Kapuskasing uplift on the Canadian Shield. This region had a high thermal gradient at that time because there was significant radioactive heat generation in the deep crust. I am aware of no example constrained by mantle xenolith geotherms.

6. Discussion, Geochemical Implications, and Conclusions

[63] The main conclusion of this paper is that the lower continental lithosphere is an effective trap for ascending kimberlite magmas and hence a globally important reservoir for CO_2. The result depends on geochemistry, specifically that the current (and past) mantle adiabat is hot enough that material ascending beneath cratons and platforms melts and liberates kimberlitic magmas. These rocks pond and freeze within the deep lithosphere, as dikes typically do not penetrate the zone of strong horizontal compression at midlithospheric depths. Considering the physics of convention constrains the rate of kimberlite production and hence its total accumulation in the deep lithosphere over the last ~2 Ga. Specifically stagnant lid convection has circulated the mass of the mantle beneath continents over that time. However, the rate that mantle-wide flow delivers undepleted material to the upper asthenosphere (and then to stagnant lid convection) limits the total fraction of the mantle that actually produced kimberlites to ~1/2. The deep lithospheric reservoir is thus ~1/2 of the mantle reservoir, $\sim 5000 \times 10^{18}$ moles (or 43 bars equivalent atmospheric pressure).

[64] This conclusion is new and has implications with respect to other subfields of mantle chemistry, geophysics, and even biology. In the remainder of this section, I provide qualitative discussion of such inferences along with the geochemical basis of this paper with the intent of facilitating quantitative study.

[65] The ascent of kimberlites (*sensu lato*) takes hours to days [e.g., *Anderson*, 1979; *Spera*, 1984; *Kelley and Wartho*, 2000; *Peslier et al.*, 2008]. Yet the natural tendency to regard these rocks as pristine samples of melts leaving their source region needs to be strongly avoided. Rather, systematic variations among these rocks between platforms and cratons indicate strong chemical reaction with the lithosphere [*Francis and Patterson*, 2009]. Thus, kimberlites intrude and metasomatize the lithospheric mantle [*Foley*, 2008; *De Stefano et al.*, 2009]. *Tappe et al.* [2008] provide evidence that such lithospheric dike networks remelted during rifting.

[66] The formation and movement of CO_2-rich magmas are voluminous enough to be evident even in active environments [*Dasgupta et al.*, 2009]. Extraction of CO_2-rich magmas affects the residuum that melts at ridge axes to form MORB [*Donnelly et al.*, 2004]. Deep CO_2-rich melts metasomatize overlying regions of the Hawaiian plume affecting rejuvenated stage lavas [*Dixon et al.*, 2008]. There is no obvious reason why CO_2-rich magma formed beneath continents should behave differently and remain within their source regions.

[67] Heat and mass balance indicates that the bulk of the mantle has circulated by stagnant lid through the melting zone in the subcontinental asthenosphere over geological time, which would poten-

tially liberate much of the mantle CO_2. The inference that a significant fraction of the generated melt ascends into the deep lithosphere implies that continental lithosphere is a massive CO_2 reservoir, scaling the total CO_2 now in the convecting mantle. The inference that significant CO_2 also remains in the convecting mantle provides the crude constraint that lithospheric total CO_2 should be comparable, to but somewhat less, than convecting mantle total CO_2. Then the deep continental lithosphere sequesters the equivalent to 10s of bars of atmospheric pressure ($\sim 5000 \times 10^{18}$ moles). There is enough $MgSiO_4$ in ambient mantle to store this amount in 1–2 km of equivalent thickness beneath the global continents.

[68] However, this reservoir though massive in the global CO_2 budget would have only subtle geophysical implications. An equivalent thickness of carbonatized mantle a few kilometers would have negligible effects on the geoid and produce negligible uplift. Depending on the ratio of CO_2:Th:U:K in the emplaced rocks, a few kilometer equivalent thickness of kimberlites would cause the xenolith geotherm to be curved. This effect is not resolved in data and probably precludes equivalent thicknesses of several kilometers. Note that the lithospheric reservoir is small enough that it does not significantly affect the silicate earth estimate of CO_2 by *Hirschmann and Dasgupta* [2009] and their conclusion that the core contains far more carbon than the silicate earth.

[69] Conversely, the continental mantle lithosphere cannot be a major reservoir of heat-producing elements. The Bulk Silicate Earth model provides illustration [*McDonough and Sun*, 1995]. The radioactivity in the crust and mantle produces 38 mW m^{-2} of equivalent heat flow globally. The concentration of 1% of this quantity beneath continents (40% of the Earth's surface) produces $\sim$1 mW m^{-2}. Concentration of more than a few percent of the Earth's radioactivity beneath continents would cause xenolith geotherms to be noticeably curved, which again is not observed. The temptation to postulate that the deep continental lithosphere is an important "hidden" reservoir for elements that behave like U and Th should be avoided without supporting evidence.

[70] Sophisticated geochemical and isotopic studies remain the best way to constrain the extent of kimberlite intrusion and carbonate metasomatism in the continental lithosphere. These studies are complicated because the mantle is heterogeneous. Subducted carbonatized oceanic crust is an obvious source domain [e.g., *Hoernle et al.*, 2002; *Zartman and Richardson*, 2005]. Subducted organic-rich sediments are obvious reducing domains. Studies of diamond inclusions indicate that these domains entered the lower mantle before ascending into the asthenosphere [e.g., *Hayman et al.*, 2005; *Walter et al.*, 2008; *Cayzer et al.*, 2008]. Magma bodies that freeze on the flanks of major ridge and plume upwellings are secondary source domains [*Donnelly et al.*, 2004; *Dixon et al.*, 2008].

[71] The presence of these multiple reservoirs precludes a simple-minded analysis using $^{13}C/^{12}C$ variations. Qualitatively, the bulk silicate earth $^{13}C/^{12}C$ needs to be "near" the meteorite value. The MORB mantle and crustal reservoirs are "near" that value. The deep lithospheric carbon reservoir can be a significant fraction of the convecting mantle reservoir (as assumed here) without violating this constraint. It cannot greatly exceed the convecting mantle reservoir if its $^{13}C/^{12}C$ is close to that of marine carbonates.

[72] The increase in the U/Th in kimberlites over the last 2.5 Ga indicates the importance of slab carbonates, confirms the reality of deep subduction, and provides a mantle biosignature of photosynthesis [*Zartman and Richardson*, 2005]. Uranium is mobile relative to thorium in oxidized continental weathering environments, but behaves similarly under reducing conditions. The oxygen concentration in the air and hence the selective delivery of U to the deep sea have increased over geological time. Sulfur isotope systematics indicate that oxygen became present in ppm quantities in the atmosphere and hence the shallow ocean at $\sim$2.45 Ga [e.g., *Kaufman et al.*, 2007; *Farquhar et al.*, 2007]. The deep ocean became suboxic by $\sim$1.8 Ga [*Slack et al.*, 2007, 2009].

[73] The high mobility of dissolved total CO_2 in seawater allows high concentrations of carbonate to accumulate within oceanic crust near ridge axes [*Sleep and Zahnle*, 2001]. The ratio of CO_2 to other incompatible elements including U, Th, and Nb in carbonatized crust is thus likely to exceed the bulk mantle average. Therefore kimberlites formed at the expense of mantle CO_2-rich domains can carry a significant fraction of the Earth's (bulk silicate) carbon inventory without greatly enriching the lithosphere in heat-producing elements. Over geological time, the bulk of the Earth's crustal and mantle carbon has passed through carbonates in the oceanic crust [e.g., *Hirschmann and Dasgupta*, 2009].

[74] The same argument applies to water in primary kimberlite melts. The carbonatized layer 2A has a small (~0.5 km) while oceanic crust is hydrated over a larger depth range. Layer 2A is near the top of the slab and preferentially dehydrated beneath arcs. Care is thus needed to estimate the water concentration in a kimberlite leaving its source region from the composition of sampled rocks. This task and the fate of water from kimberlites that freeze in the deep lithosphere is beyond the scope of this paper.

[75] The processes that lead to kimberlites should have varied over geological time. Warm systems (those that vent water at 10s of degrees Celsius) occur on young ~1 Ma crust and quantitatively consume the CO_2 that enters them [*Sleep and Zahnle*, 2001]. Almost all oceanic crust eventually subducts. Comparable fractions of the slab carbonate vent to the surface at island arcs and continue into the deep mantle. The flux of carbonate into the deep mantle is thus proportional to the global spreading rate and the concentration of total CO_2 in seawater and hence CO_2 in the air.

[76] The CO_2 concentration in air has been variable over the Phanerozoic Eon [*Ekart et al.*, 1999], but overall has likely declined over the last 2.5 Ga, as the mass of platform carbonates increased [*Sleep and Zahnle*, 2001, and references therein]. Carbonated crust has been subducted (*sensu lato*) since the aftermath of the moon-forming impact at ~4.5 Ga [*Sleep et al.*, 2001]. One might expect chemical differences between subducted carbonate hosted by basalt, slow ridge serpentinite, hypersaline oceanic crust from narrow nascent ocean basins like the Red Sea, komatiite oceanic crust, and peridotitic ejecta from asteroid impacts. The temperature of the mantle through which the slab passed at subduction zones should have some effect arc magma extraction and hence on the eventual kimberlites. Further inference of systematic changes in subducted carbonate over time and recognizing specific source protoliths for individual kimberlites by their effects on kimberlitic melts are beyond the scope of this paper even though it would constrain the behavior of tectonics over geological time.

[77] Mechanically, kimberlites can repeatedly intrude into and accumulate within the deep lithosphere because stresses from an intrusion relax quickly on a geological time scale permitting subsequent intrusions. The nearly rigid uppermost mantle lithosphere is typically in horizontal compression. Kimberlites that make it to that level usually turn into horizontal sills and do not often breach the crust.

[78] The issue of whether kimberlites are associated with plumes arises [e.g., *Le Roex*, 1986; *Heaman and Kjargaard*, 2000]. Obviously, hot mantle should produce more voluminous melts than ordinary mantle and hot voluminous magma is less likely to freeze on the way up than meager cold magma. However, the effect of buoyant plume material ponded at the base of the lithosphere may be more important as it tends to put the lithosphere under horizontal tension so that dikes can ascend to the surface.

Acknowledgments

[79] This research was in part supported by NSF grant EAR-0000747. Don Francis pointed out the issue of lithospheric carbonates and provided preprint of his paper. Marc Hirschmann provided preprint of his paper and helpful comments. John Slack pointed out data on the oxidation state of the deep ocean. Claude Jaupart and an anonymous reviewer provided helpful comments including the need to explicitly consider mantle-wide flow. David Snyder sent a preprint of his paper.

References

Anderson, O. L. (1979), The role of fracture dynamics in kimberlite pipe formation, in *Kimberlites, Diatremes, and Diamonds: Their Geology, Petrology, and Geochemistry*, edited by F. R. Boyd and H. O. A. Meyer, pp. 344–353, AGU, Washington, D. C.

Artemieva, I. M., and W. D. Mooney (2001), Thermal thickness and evolution of Precambrian lithosphere: A global study, *J. Geophys. Res.*, *106*, 16,387–16,414, doi:10.1029/2000JB900439.

Asimow, P. D. (2002), Steady-state mantle-melt interactions in one dimension: II. Thermal interactions and irreversible terms, *J. Petrol.*, *43*, 1707–1724, doi:10.1093/petrology/43.9.1707.

Bass, J. D. (1995), Elasticity of mineral, glasses, and melts, in *A Handbook of Physical Constants*, *AGU Ref. Shelf*, vol. 2, edited by T. J. Ahrens, pp. 45–63, AGU, Washington, D. C.

Bunge, H.-P. (2005), Low plume excess temperature and high core heat flux inferred from non-adiabatic geotherms in internally heated mantle circulation models, *Phys. Earth Planet. Inter.*, *153*, 3–10, doi:10.1016/j.pepi.2005.03.017.

Calais, E., J. Y. Han, C. DeMets, and J. M. Nocquet (2006), Deformation of the North American plate interior from a decade of continuous GPS measurements, *J. Geophys. Res.*, *111*, B06402, doi:10.1029/2005JB004253.

Canil, D. (1990), Experimental-study bearing on the absence of carbonate in mantle-derived xenoliths, *Geology*, *18*, 1011–1013, doi:10.1130/0091-7613(1990)018<1011:ESBOTA>2.3.CO;2.

Cartigny, P., F. Pineau, C. Aubaud, and M. Javoy (2008), Towards a consistent mantle carbon flux estimate: Insights from volatile systematics (H_2O/Ce, ∂D, CO_2/Nb) in the North Atlantic mantle (14°N and 34°N), *Earth Planet. Sci. Lett.*, *265*, 672–685, doi:10.1016/j.epsl.2007.11.011.

Cayzer, N. J., S. Odake, B. Harte, and H. Kagi (2008), Plastic deformation of lower mantle diamonds by inclusion phase transformations, *Eur. J. Mineral.*, *20*(3), 333–339, doi:10.1127/0935-1221/2008/0020-1811.

Cookenboo, H. O. (1999), History and process of emplacement of the Jericho (JD-1) kimberlite pipe, northern Canada, in *The Dawson Volume, Proceedings of the VIIth International Kimberlite Conference*, edited by J. J. Gurney et al., pp. 125–133, Red Roof Design, Cape Town, South Africa.

Dasgupta, R., and M. M. Hirschmann (2007), Effect of variable carbonate concentration on the solidus of mantle peridotite, *Am. Mineral.*, *92*, 370–379, doi:10.2138/am.2007.2201.

Dasgupta, R., M. M. Hirschmann, W. F. McDonough, M. Spiegelman, and A. C. Withers (2009), Trace element partitioning between garnet lherzolite and carbonatite at 6.6 and 8.6 GPa with applications to the geochemistry of the mantle and of mantle-derived melts, *Chem. Geol.*, *262*, 57–77, doi:10.1016/j.chemgeo.2009.02.004.

Davaille, A., and C. Jaupart (1993a), Thermal convection in lava lakes, *Geophys. Res. Lett.*, *20*, 1827–1830, doi:10.1029/93GL02008.

Davaille, A., and C. Jaupart (1993b), Transient high-Rayleigh-number thermal convection with large viscosity variations, *J. Fluid Mech.*, *253*, 141–166, doi:10.1017/S0022112093001740.

Davaille, A., and C. Jaupart (1994), The onset of thermal convection in fluids with temperature-dependent viscosity: Application to the oceanic mantle, *J. Geophys. Res.*, *99*, 19,853–19,866, doi:10.1029/94JB01405.

Davis, G. L. (1977), The ages and uranium contents of zircons from kimberlites and associated rocks, *Year Book Carnegie Inst. Washington*, *76*, 631–635.

De Stefano, A., M. G. Kopyova, P. Cartigny, and V. Afanasiey (2009), Diamonds and eclogites of the Jericho kimberlite (northern Canada), *Contrib. Mineral. Petrol.*, *158*, 295–315, doi:10.1007/s00410-009-0384-7.

Dixon, J., D. A. Clague, B. Cousens, M. L. Monsalve, and J. Uhl (2008), Carbonatite and silicate melt metasomatism of the mantle surrounding the Hawaiian plume: Evidence from volatiles, trace elements, and radiogenic isotopes in rejuvenated-stage lavas from Niihau, Hawaii, *Geochem. Geophys. Geosyst.*, *9*, Q09005, doi:10.1029/2008GC002076.

Doin, M.-P., L. Fleitout, and U. Christensen (1997), Mantle convection and stability of depleted and undepleted continental lithosphere, *J. Geophys. Res.*, *102*, 2771–2787, doi:10.1029/96JB03271.

Donnelly, K. E., S. L. Goldstein, C. H. Langmuir, and M. Spiegelman (2004), Origin of enriched ocean ridge basalts and implications for mantle dynamics, *Earth Planet. Sci. Lett.*, *226*, 347–366, doi:10.1016/j.epsl.2004.07.019.

Ekart, D. D., T. E. Cerling, I. P. Montañez, and N. J. Tabor (1999), A 400 million year carbon isotopic record of pedogenic carbonate: Implications for paleoatmospheric carbon dioxide, *Am. J. Sci.*, *299*, 805–827, doi:10.2475/ajs.299.10.805.

Farquhar, J., M. Peters, D. T. Johnston, H. Strauss, A. Masterson, U. Wiechert, and A. J. Kaufman (2007), Isotopic evidence for Mesoarchaean anoxia and changing atmospheric sulphur chemistry, *Nature*, *449*, 706–709, doi:10.1038/nature06202.

Foley, S. L. (2008), Rejuvenation and erosion of the cratonic lithosphere, *Nat. Geosci.*, *1*, 503–519, doi:10.1038/ngeo261.

Francis, D., and M. Patterson (2009), Kimberlites and aillikites as probes of the continental lithospheric mantle, *Lithos*, *109*, 72–80, doi:10.1016/j.lithos.2008.05.007.

Frost, D. J., and C. A. McCammon (2008), The redox state of Earth's mantle, *Annu. Rev. Earth Planet. Sci.*, *36*, 389–420, doi:10.1146/annurev.earth.36.031207.124322.

Gaillard, F., M. Malki, G. Iacono-Marziano, M. Pichavant, and B. Scaillet (2008), Carbonatite melts and electrical conductivity in the asthenosphere, *Science*, *322*, 1363–1365, doi:10.1126/science.1164446.

Griffin, W. L., S. Y. O'Reilly, and C. G. Ryan (1999), The composition and origin of sub-continental mantle, in *Mantle Petrology: Field Observations and High Pressure Experimentation: A Tribute to Francis R. (Joe) Boyd*, edited by Y. Fei, C. M. Bertka, and B. O. Mysen, *Spec. Publ. Geochem. Soc.*, *6*, 13–45.

Hayman, P. C., M. G. Kopylova, and F. V. Kaminsky (2005), Lower mantle diamonds from Rio Soriso (Juina area, Mato Grosso, Brazil), *Contrib. Mineral. Petrol.*, *149*, 430–445, doi:10.1007/s00410-005-0657-8.

Heaman, L. M., and B. A. Kjargaard (2000), Timing of eastern North American kimberlite magmatism: Continental extension of the Great Meteor hotspot track, *Earth Planet. Sci. Lett.*, *178*, 253–268, doi:10.1016/S0012-821X(00)00079-0.

Hirschmann, M. M., and R. Dasgupta (2009), The H/C ratios of Earth's near surface and deep reservoirs, and the consequences for deep Earth volatile cycles, *Chem. Geol.*, *262*, 4–16, doi:10.1016/j.chemgeo.2009.02.008.

Hoernle, K., G. Tilton, M. J. Le Bas, S. Duggen, and D. Garbe-Schönberg (2002), Geochemistry of oceanic carbonatites compared with continental carbonatites: Mantle recycling of oceanic crustal carbonate, *Contrib. Mineral. Petrol.*, *142*, 520–542, doi:10.1007/s004100100308.

Holser, W. T., M. Schidlowski, F. T. Mackenzie, and J. B. Maynard (1988), Geochemical cycles of carbon and sulfur, in *Chemical Cycles in the Evolution of the Earth*, edited by C. B. Gregor et al., pp. 105–173, John Wiley, New York.

Jaupart, C., and J. C. Mareschal (1999), The thermal structure and thickness of continental roots, *Lithos*, *48*, 93–114, doi:10.1016/S0024-4937(99)00023-7.

Jaupart, C., J. C. Mareschal, L. Guillou-Frottier, and A. Davaille (1998), Heat flow and thickness of the lithosphere in the Canadian Shield, *J. Geophys. Res.*, *103*, 15,269–15,286, doi:10.1029/98JB01395.

Kaufman, A. J., et al. (2007), Late Archean biospheric oxygenation and atmospheric evolution, *Science*, *317*, 1900–1903, doi:10.1126/science.1138700.

Kelley, S. P., and J. A. Wartho (2000), Rapid kimberlite ascent and the significance of Ar-Ar ages in xenolith phlogopites, *Science*, *289*, 609–611, doi:10.1126/science.289.5479.609.

Kopylova, M. G., J. K. Russell, and H. O. Cookenboo (1999a), Mapping the lithosphere beneath the north central Slave Craton, in *The Dawson Volume, Proceedings of the VIIth International Kimberlite Conference*, edited by J. J. Gurney et al., pp. 468–479, Red Roof Design, Cape Town, South Africa.

Kopylova, M. G., J. K. Russell, and H. Cookenboo (1999b), Petrolgy of peridotite and pyroxenite xenoliths from the Jericho kimberlite: Implications for the thermal state of the mantle beneath the Slave craton: Northern Canada, *J. Petrol.*, *40*, 79–104, doi:10.1093/petrology/40.1.79.

Le Roex, A. P. (1986), Geochemical correlation between southern African kimberlites and South Atlantic hotspots, *Nature*, *324*, 243–245, doi:10.1038/324243a0.

McDonough, W. F., and S. Sun (1995), The composition of the Earth, *Chem. Geol.*, *120*, 223–253, doi:10.1016/0009-2541(94)00140-4.

McKenzie, D. P. (1984), The generation and compaction of partial melts, *J. Petrol.*, *25*, 713–765.

McKenzie, D. P., and M. J. Bickle (1988), The volume and composition of melt generated by extension of the lithosphere, *J. Petrol.*, *29*, 625–679.

Moore, A. E., and N. P. Lock (2001), The origin of mantle-derived magacrysts and sheared peridotite from kimberlites in the northern Lesotho Orange Free State (South Africa) and Botswana pipe clusters, *S. Afr. J. Geol.*, *104*, 23–38, doi:10.2113/104.1.23.

Perry, H. K. C., J. C. Mareschal, and C. Jaupart (2006), Variations of strength and localized deformation in cratons: The 1.9 Ga Kapuskasing uplift, Superior Province, Canada, *Earth Planet. Sci. Lett.*, *249*, 216–228, doi:10.1016/j.epsl.2006.07.013.

Peslier, A. H., A. B. Woodland, and J. A. Wolf (2008), Fast kimberlite ascent rates estimated from hydrogen diffusion profiles in xenolithic mantle olivines from southern Africa, *Geochim. Cosmochim. Acta*, *72*(11), 2711–2722, doi:10.1016/j.gca.2008.03.019.

Plank, T., and C. H. Langmuir (1992), Effects of the melting regime on the composition of the oceanic crust, *J. Geophys. Res.*, *97*(B13), 19,749–19,770, doi:10.1029/92JB01769.

Price, S. E., J. K. Russell, and M. G. Kopylova (2000), Primitive magma from the Jericho pipe, NWT, Canada: Constraints on primary melt chemistry, *J. Petrol.*, *41*, 789–808, doi:10.1093/petrology/41.6.789.

Saal, A. E., E. H. Hauri, C. H. Langmuir, and M. R. Perfitt (2002), Vapour undersaturation in primitive mid-ocean-ridge basalt and the volatile content of the Earth's upper mantle, *Nature*, *419*, 451–455, doi:10.1038/nature01073.

Sano, Y., and S. N. Williams (1996), Fluxes of mantle and subducted carbon along convergent plate boundaries, *Geophys. Res. Lett.*, *23*, 2749–2752, doi:10.1029/96GL02260.

Shapiro, S. S., B. H. Hager, and T. H. Jordan (1999a), The continental tectosphere and Earth's long-wavelength gravity field, *Lithos*, *48*, 135–152, doi:10.1016/S0024-4937(99)00027-4.

Shapiro, S. S., B. H. Hager, and T. H. Jordan (1999b), Stability and dynamics of the continental tectosphere, *Lithos*, *48*, 115–133, doi:10.1016/S0024-4937(99)00025-0.

Slack, J. F., T. Grenne, A. Bekker, O. J. Rouxel, and P. A. Lindberg (2007), Suboxic deep seawater in the late Paleoproterozoic: Evidence from hematitic chert and iron formation related to seafloor-hydrothermal sulfide deposits, central Arizona, USA, *Earth Planet. Sci. Lett.*, *255*, 243–256, doi:10.1016/j.epsl.2006.12.018.

Slack, J. F., T. Grenne, and A. Bekker (2009), Seafloor-hydrothermal Si-Fe-Mn exhalites in the Pecos greenstone belt, New Mexico, and the redox state of ca. 1720 Ma deep seawater, *Geosphere*, *5*(3), 302–314, doi:10.1130/GES00220.1.

Sleep, N. H. (2003a), Geodynamic implications of xenolith geotherms, *Geochem. Geophys. Geosyst.*, *4*(9), 1079, doi:10.1029/2003GC000511.

Sleep, N. H. (2003b), Survival of Archean cratonal lithosphere, *J. Geophys. Res.*, *108*(B6), 2302, doi:10.1029/2001JB000169.

Sleep, N. H., and A. M. Jellinek (2008), Scaling relationships for chemical lid convection with applications to cratonal lithosphere, *Geochem. Geophys. Geosyst.*, *9*, Q12025, doi:10.1029/2008GC002042.

Sleep, N. H., and K. Zahnle (2001), Carbon dioxide cycling and implications for climate on ancient Earth, *J. Geophys. Res.*, *106*, 1373–1399, doi:10.1029/2000JE001247.

Sleep, N. H., and M. D. Zoback (2007), Did earthquakes keep the early crust habitable?, *Astrobiology*, *7*(6), 1023–1032, doi:10.1089/ast.2006.0091.

Sleep, N. H., K. Zahnle, and P. S. Neuhoff (2001), Initiation of clement surface conditions on the early Earth, *Proc. Natl. Acad. Sci. U. S. A.*, *98*, 3666–3672, doi:10.1073/pnas.071045698.

Smyth, J. R., and T. C. McCormick (1995), Crystallographic data for minerals, in *Mineral Physics and Crystallography: A Handbook of Physical Constants*, *AGU Ref. Shelf*, vol. 2, edited by T. J. Ahrens, pp. 1–17, AGU, Washington, D. C.

Snyder, D. B., and G. Lockhart (2009), Does seismically anisotropic subcontinental mantle lithosphere require metasomatic wehrlite–pyroxenite dyke stockworks?, *Lithos*, doi:10.1016/j.lithos.2009.03.033, in press.

Solomatov, V. S. (1995), Scaling of temperature- and stress-dependent viscosity convection, *Phys. Fluids*, *7*, 266–274, doi:10.1063/1.868624.

Solomatov, V. S., and L.-N. Moresi (2000), Scaling of time-dependent stagnant lid convection: Application to small-scale convection on Earth and other terrestrial planets, *J. Geophys. Res.*, *105*, 21,795–21,817, doi:10.1029/2000JB900197.

Spera, F. J. (1984), Carbon-dioxide in petrogenesis III: Role of volatiles in the ascent of alkaline magma with special reference to xenolith-bearing mafic lavas, *Contrib. Mineral. Petrol.*, *88*, 217–232, doi:10.1007/BF00380167.

Tappe, S., S. F. Foley, B. A. Kjarsgaard, R. L. Romer, L. M. Heaman, A. Stracke, and G. A. Jenner (2008), Between carbonatite and lamproite—Diamondiferous Torngat ultramafic lamprophyres formed by carbonate-fluxed melting of cratonic MARID-type metasomes, *Geochim. Cosmochim. Acta*, *72*, 3258–3286, doi:10.1016/j.gca.2008.03.008.

Upadhyay, D., E. E. Scherer, and K. Mezger (2009), ^{142}Nd evidence for an enriched Hadean reservoir in cratonic roots, *Nature*, *459*, 1118–1121, doi:10.1038/nature08089.

Walter, M. J., et al. (2008), Primary carbonatite melt from deeply subducted oceanic crust, *Nature*, *454*(7204), 622–630, doi:10.1038/nature07132.

Zahnle, K., N. Arndt, C. Cockell, A. Halliday, E. Nisbet, F. Selsis, and N. H. Sleep (2007), Emergence of a habitable planet, *Space Sci. Rev.*, *129*, 35–78, doi:10.1007/s11214-007-9225-z.

Zartman, R. E., and S. H. Richardson (2005), Evidence from kimberlitic zircon for a decreasing mantle Th/U since the Archean, *Chem. Geol.*, *220*, 263–283, doi:10.1016/j.chemgeo.2005.04.003.

Zoback, M. D., and J. Townend (2001), Implications of hydrostatic pore pressures and high crustal strength for the deformation of intraplate lithosphere, *Tectonophysics*, *336*, 19–30, doi:10.1016/S0040-1951(01)00091-9.

Zoback, M. L., et al. (1989), Global patterns of tectonic stress, *Nature*, *341*, 291–298, doi:10.1038/341291a0.

Zoback, M. D., J. Townend, and B. Grollimund (2002), Steady-state failure equilibrium and deformation of intraplate lithosphere, *Int. Geol. Rev.*, *44*, 383–401, doi:10.2747/0020-6814.44.5.383.